Evanescent and inertial-like waves in rigidly-rotating odd viscous liquids - Supplementary Materials

E. Kirkinis† and M. Olvera de la Cruz

Department of Materials Science & Engineering, Robert R. McCormick School of Engineering and Applied Science, Northwestern University , Evanston IL 60208 USA
Center for Computation and Theory of Soft Materials, Northwestern University , Evanston IL 60208 USA

We provide some illustrative examples of the axisymmetric case ($m = 0$) and a discussion of plane polarized waves in two-dimensional compressible and three-dimensional incompressible odd viscous liquids.

S-I. Inertial-like waves in a three dimensional rigidly-rotating incompressible odd viscous liquid

Consider an inviscid odd viscous liquid rotating rigidly about the $\hat{\mathbf{z}}$ axis with angular velocity Ω (cf. Fig. S-I). For an axially symmetric wave propagating along the axis the time and axial dependence are given by the factor $\exp[i(kz-\omega t)]$ where the frequency ω and wave number k along the axis are both real. We consider cylindrical polar coordinates r, ϕ, z, and fields that are independent of ϕ. We neglect the nonlinear terms by assuming small-amplitude motions. The odd viscous stress in polar cylindrical coordinates (cf. Fig. S-I) associated with one of the odd viscosity coefficients (we refer the reader to (Kirkinis & Olvera de la Cruz 2023) for the general form) is of the form

$$\boldsymbol{\sigma}' = \eta_o \begin{pmatrix} -\left(\partial_r v_\phi - \frac{1}{r} v_\phi + \frac{1}{r}\partial_\phi v_r\right) & \partial_r v_r - \frac{1}{r} v_r - \frac{1}{r}\partial_\phi v_\phi & 0 \\ \partial_r v_r - \frac{1}{r} v_r - \frac{1}{r}\partial_\phi v_\phi & \partial_r v_\phi - \frac{1}{r} v_\phi + \frac{1}{r}\partial_\phi v_r & 0 \\ 0 & 0 & 0 \end{pmatrix}, \tag{S1}$$

where $\eta_o(>0)$ is the coefficient of dynamic odd viscosity. Here the liquid is three-dimensional, and the velocity field satisfies the incompressibility condition

$$\partial_r(r v_r) + r\partial_z v_z = 0. \tag{S2}$$

The constitutive law (S1) implies that an axis of anisotropy has, by some fortuitous mechanism, been established pointing in the $\hat{\mathbf{z}}$ direction.

The Navier-Stokes equations take the form

$$-i\omega v_r - 2\Omega v_\phi = -\frac{1}{\rho}\frac{\partial p'}{\partial r} - \nu_o\left[\frac{1}{r}\frac{\partial}{\partial r}\left(r\frac{\partial v_\phi}{\partial r}\right) - \frac{v_\phi}{r^2}\right], \tag{S3}$$

$$-i\omega v_\phi + 2\Omega v_r = \nu_o\left[\frac{1}{r}\frac{\partial}{\partial r}\left(r\frac{\partial v_r}{\partial r}\right) - \frac{v_r}{r^2}\right], \tag{S4}$$

$$-i\omega v_z = -\frac{ik}{\rho}p', \tag{S5}$$

† Email address for correspondence: kirkinis@northwestern.edu

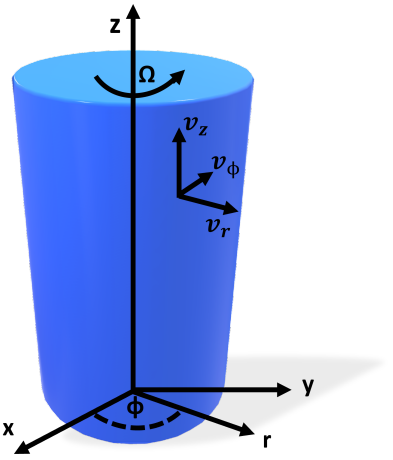

Figure S-I: Three-dimensional odd viscous liquid rotating with angular velocity Ω about the $\hat{\mathbf{z}}$ axis. In cylindrical coordinates the velocity field is $\mathbf{v} = v_r\hat{\mathbf{r}} + v_\phi\hat{\boldsymbol{\phi}} + v_z\hat{\mathbf{z}}$ in the frame of reference rotating with the liquid.

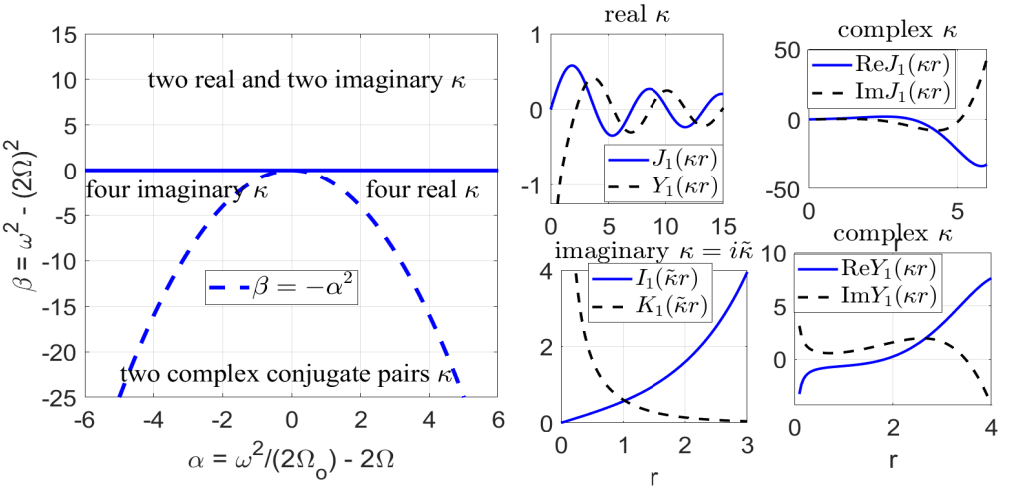

Figure S-II: Left panel: Roots of Eq. (S12) & (S14) in the parameter space (α, β) defined in Eq. (S13). In the absence of rotation ($\Omega = 0$, so $\beta > 0$) only the two real and two imaginary roots are possible as discussed in Kirkinis & Olvera de la Cruz (2023). Rich behavior exists in the presence of rotation. This includes the oscillatory Bessel functions for real κ, exponentially increasing/decreasing Bessel functions for κ imaginary and exponential-oscillating Bessel functions for complex κ. These behaviors are displayed in the right four panels where arbitrary units are employed.

where p' is the variable part of the pressure in the wave and $\nu_o \equiv \eta_o/\rho$ is the coefficient of kinematic odd viscosity. The incompressibility condition (S2) becomes

$$\frac{1}{r}\frac{\partial}{\partial r}(rv_r) + ikv_z = 0. \tag{S6}$$

It is possible to simplify system (S3)-(S5). Combining Eq. (S5) and (S6) we obtain $p'/\rho =$

$\alpha^2+\beta$	α	β	Type of root κ
+		+	two real, two imaginary
+	+	−	four real
+	−	−	four imaginary
−			two complex conjugate pairs

Table S-I: Types of roots κ from Eq. (S12)/(S14) $\nu_o\kappa^2 = \alpha \pm \sqrt{\alpha^2+\beta}$ according to the sign of the parameters $\alpha = \frac{\omega^2}{2\Omega_o} - 2\Omega$ and $\beta = \omega^2 - (2\Omega)^2$ defined in Eq. (S13)

$\omega v_z/k = \frac{i\omega}{k^2}\frac{1}{r}\frac{\partial}{\partial r}(rv_r)$. Employing the identity $\frac{\partial}{\partial r}\left(\frac{1}{r}\frac{\partial}{\partial r}(rv_r)\right) = \frac{1}{r}\frac{\partial}{\partial r}\left(r\frac{\partial v_r}{\partial r}\right) - \frac{v_r}{r^2}$, leads to an expression we will susbstitute into (S3): $\frac{1}{\rho}\frac{\partial p'}{\partial r} = \frac{i\omega}{k^2}\left[\frac{1}{r}\frac{\partial}{\partial r}\left(r\frac{\partial v_r}{\partial r}\right) - \frac{v_r}{r^2}\right]$.

The expressions $\frac{1}{r}\frac{\partial}{\partial r}\left(r\frac{\partial}{\partial r}\right) - \frac{1}{r^2}$ appearing in the square brackets of (S3) and (S4) can be replaced by

$$\mathcal{L} = \partial_r^2 + \frac{1}{r}\partial_r - \frac{1}{r^2}. \tag{S7}$$

Thus, the r and ϕ momentum equations become

$$-i\omega v_r = -i\frac{\omega}{k^2}\mathcal{L}v_r - (\nu_o\mathcal{L} - 2\Omega)\, v_\phi, \tag{S8}$$

$$-i\omega v_\phi = (\nu_o\mathcal{L} - 2\Omega)\, v_r. \tag{S9}$$

Expressing the velocities v_r and v_ϕ in terms of Bessel functions, $v_r = AJ_1(\kappa r), v_\phi = BJ_1(\kappa r)$, etc., (where A and B are constants to be determined by the boundary conditions and κ is an eigenvalue) the system (S8) and (S9) has a solution when the determinant of the coefficients of the resulting linear system

$$\frac{i\left(\nu_o\kappa^2 + 2\Omega\right)B\,k^2 - A\,\kappa^2\omega}{k^2\omega} - A = 0, \quad -\frac{iA\left(\nu_o\kappa^2 + 2\Omega\right)}{\omega} - B = 0, \tag{S10}$$

vanishes. This leads to a quartic equation for the determination of κ

$$-\kappa^4k^2\nu_o^2 + \left(-4\Omega\,k^2\nu_o + \omega^2\right)\kappa^2 - (2\Omega - \omega)(2\Omega + \omega)\,k^2 = 0, \tag{S11}$$

with solutions

$$\kappa = \left[\frac{-4\Omega\,k^2\nu_o + \omega^2 \pm \sqrt{4k^4\nu_o^2\omega^2 - 8\Omega\,k^2\nu_o\,\omega^2 + \omega^4}}{2\nu_o^2k^2}\right]^{1/2}. \tag{S12}$$

Here the frequency ω and wave number k along the axis are both real quantities. κ can be real, imaginary or complex and it is this behavior of κ that gives rise to the diverse character of the velocity fields discussed in this paper.

To understand the structure of solutions we define an "odd" frequency and cumulative (frequency and frequency squared, respectively) parameters α and β of the form

$$\Omega_o = \nu_o k^2, \quad \alpha = \frac{\omega^2}{2\Omega_o} - 2\Omega, \quad \beta = \omega^2 - (2\Omega)^2. \tag{S13}$$

With this notation Eq. (S12) becomes

$$\nu_o\kappa^2 = \frac{\omega^2}{2\Omega_o} - 2\Omega \pm \sqrt{\left(\frac{\omega^2}{2\Omega_o} - 2\Omega\right)^2 + \omega^2 - (2\Omega)^2} \equiv \alpha \pm \sqrt{\alpha^2+\beta}. \tag{S14}$$

Velocity fields obtained according to the type of κ are displayed in Fig. S-II and Table

S-I. Their functional form is

$$v_r = AJ_1(\kappa r)e^{i(kz-\omega t)}, \quad v_\phi = -iA\frac{\nu_o\kappa^2+2\Omega}{\omega}J_1(\kappa r)e^{i(kz-\omega t)}, \quad v_z = iA\frac{\kappa}{k}J_0(\kappa r)e^{i(kz-\omega t)}. \tag{S15}$$

When the type of the eigenvalue κ has been decided upon, one can write down the dispersion relation

$$\omega = \pm\frac{k\left(\nu_o\,\kappa^2+2\Omega\right)}{\sqrt{k^2+\kappa^2}} \tag{S16}$$

which becomes nonconvex when $\nu_o\Omega<0$ and κ is real, and can thus be associated with unconventional behavior when nonlinear terms are included. A detailed discussion of this point is delegated to the polarized inertial wave section S-IV and to its two-dimensional counterpart in section S-VI.2.

S-II. Illustrative examples

S-II.1. *Oscillating inertial waves*

Consider the case where $\omega\sim 2\Omega$ and thus $\nu_o\kappa^2\sim 2\alpha = 4\Omega\left(\frac{\Omega}{\Omega_o}-1\right)$ or $\nu_o\kappa^2=0$ from Eq. (S14). Two real roots exist as long as $\Omega>\Omega_o\equiv\nu_o k^2$ and the velocity field is given by (S15). This motion comprises regions between concentric cylinders of radius r_n such that

$$r_n\kappa = \gamma_n \tag{S1}$$

and γ_n are the zeros of $J_1(x)$. Both v_r and v_ϕ vanish at these cocentric circles and the fluid does not cross them. This case resembles one in (Kirkinis & Olvera de la Cruz 2023) and we only include the final results. We consider a liquid enclosed in a cylinder of radius $r=b$. This boundary will be a streamline located at an integral number of cells in the radial direction. Writing down the streamfunction

$$\psi(r,z) = \frac{\kappa}{3.83}rJ_1(\kappa r)\sin(kz), \quad v_z = \frac{1}{r}\frac{\partial\psi}{\partial r}, \quad v_r = -\frac{1}{r}\frac{\partial\psi}{\partial z}, \tag{S2}$$

we display the instantaneous streamlines in Fig. S-III where we chose $\kappa b=\gamma_2\sim 7.0156$, the latter being the second zero of $J_1(x)$. Here the amplitude is modulated by the first zero of the Bessel function $J_1(x)$ in a manner analogous to the rigidly-rotating case of a (non-odd) viscous liquid Fig. 7.6.4 of (Batchelor 1967, p.561).

S-III. Helicity in rigidly rotating odd viscous liquids

When the roots κ of Eq. (S12) are real, one can easily show that the the vorticity of axisymmetric waves developed in section S-I is proportional to the velocity of the liquid. This generalizes the case of odd viscous liquid without rotation developed in (Kirkinis & Olvera de la Cruz 2023) and the results obtained here are identical to the non-rotating case

$$\mathrm{curl}\mathbf{v} = \mp\sqrt{k^2+\kappa^2}\mathbf{v}, \quad \text{and} \quad \mathbf{v}\cdot\mathrm{curl}\mathbf{v} = \mp\sqrt{k^2+\kappa^2}|\mathbf{v}|^2, \tag{S1}$$

with the understanding that the frequency ω in the present case satisfies the relation $\omega=\frac{(\nu_o\kappa^2+2\Omega)k}{\sqrt{k^2+\kappa^2}}$.

We now show that vorticity is parallel to the velocity when κ is imaginary (the case of evanescent waves). From Eq. (S15) with $\kappa=i\tilde{\kappa}$ imaginary and $\tilde{\kappa}$ real, we find that the

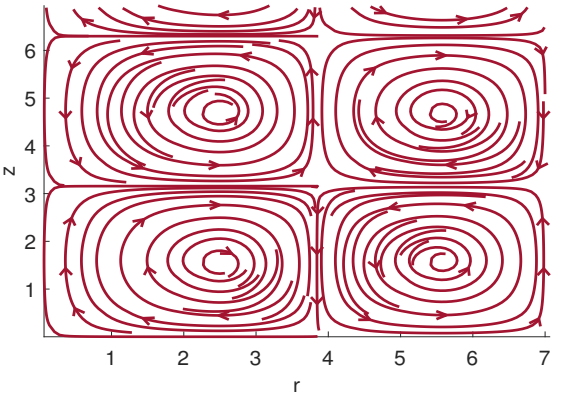

Figure S-III: Instantaneous streamlines in the $r-z$ plane with streamfunction (S2), representing a simple harmonic wave propagating in the $z-$ direction with phase velocity $c_p = \omega/k$. The line $r = 0$ is the central axis of the cylinder and the line $r = 7.0156(= b)$ is the surface of the enclosing cylinder where the radial velocity v_r vanishes (we've chosen $\kappa = 1$ in arbitrary units).

vorticity

$$\mathrm{curl}\mathbf{v} = k\frac{\nu_o\tilde{\kappa}^2 - 2\Omega}{\omega}v_r\hat{\mathbf{r}} + \frac{\omega}{\nu_o\tilde{\kappa}^2 - 2\Omega}\frac{k^2 - \tilde{\kappa}^2}{k}v_\phi\hat{\boldsymbol{\phi}} + k\frac{\nu_o\tilde{\kappa}^2 - 2\Omega}{\omega}v_z\hat{\mathbf{z}}. \tag{S2}$$

The coefficients multiplying the velocities in (S2) are equal to each other if

$$\omega^2 = \frac{k^2(\nu_o\tilde{\kappa}^2 - 2\Omega)^2}{k^2 - \tilde{\kappa}^2} \tag{S3}$$

and this is exactly the relation we obtain from (S12) by solving for ω^2 when κ is imaginary. Eq. (S3) introduces a constraint on the wavenumbers, that is, $k^2 > \tilde{\kappa}^2$ for the frequency to remain real. Thus, overall we can write that

$$\mathrm{curl}\mathbf{v} = \mp\sqrt{k^2 - \tilde{\kappa}^2}\mathbf{v}, \quad k > \tilde{\kappa}. \tag{S4}$$

replacing $\mathrm{curl}\mathbf{v} = \mp\sqrt{k^2 + \kappa^2}\mathbf{v}$ that holds when κ as a root of (S12) is real.

S-IV. Plane-polarized waves induced in a rigidly-rotating liquid by odd viscosity

S-IV.1. *The effect of the η_o viscous stress*

Plane-polarized waves in rigidly-rotating liquids support inertial-like waves (Landau & Lifshitz 1987, §14) and (Davidson 2013). In a previous communication we showed that plane polarized waves are also supported in a (non-rotating) odd viscous liquid (Kirkinis & Olvera de la Cruz 2023). It turns out that inertial-like waves that arise when rotation and odd viscosity are combined, present some special characteristics. For instance, below we show that the group velocity develops extrema where the propagation wavevector $\mathbf{k}$ *is not* perpendicular to the rotation/anisotropy axis. This takes place when the dispersion ω has an inflection point, which coincides with the vanishing of the determinant of the matrix $\partial^2\omega/\partial k_i\partial k_j$. This implies that in such problems we are dealing with a non-convex dispersion relation. Nonconvex dispersions have been associated with the appearance of

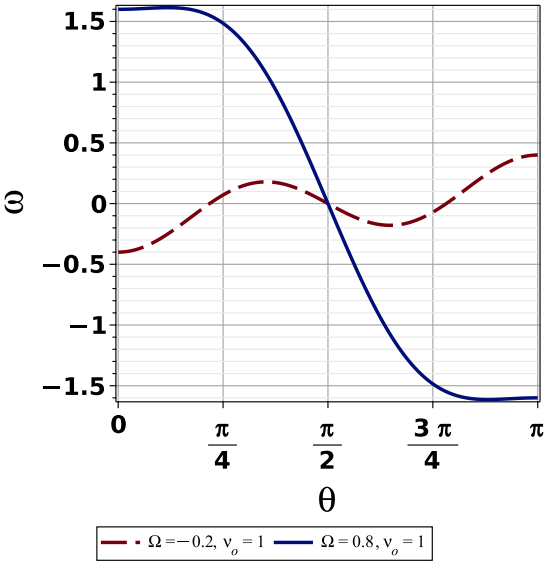

Figure S-IV: Plane-polarized wave dispersion ω (Eq. (S4)) versus angle θ between the wavevector $\mathbf{k}$ and the z- (anisotropy/rotation) axis (setting $k = \nu_o = 1$ in arbitrary units). Of interest is the dashed curve denoting the existence of non-convex dispersion for the displayed parameters. At its inflection points the group velocity becomes maximum (cf. Fig. S-V) and the second derivative $|\partial^2_{k_i k_j}\omega|$ vanishes (cf. Fig. S-VI), implying the presence of caustics and a breakdown of the longtime asymptotics.

caustics leading to self-focusing of nonlinear waves. It is thus of some interest to classify the locations at which such behavior may arise.

The linearized vorticity equation of an odd viscous liquid subject to the constitutive law (S1) obtains the form

$$\partial_t \mathrm{curl}\mathbf{v} = (2\Omega - \nu_o \nabla_2^2)\frac{\partial \mathbf{v}}{\partial z}, \tag{S1}$$

where $\nabla_2^2 = \partial_x^2 + \partial_y^2$. We seek plane-wave solutions of the form

$$\mathbf{v} = \mathbf{A}e^{i(\mathbf{k}\cdot\mathbf{r}-\omega t)}, \tag{S2}$$

which leads to the requirement that $\mathbf{A}\cdot\mathbf{k} = 0$ from the incompressibility condition.

Substituting the plane-wave solution into (S1) we obtain

$$\omega \mathbf{k}\times\mathbf{v} = i\left[2\Omega + \nu_o(k_x^2 + k_y^2)\right]k_z\mathbf{v}. \tag{S3}$$

From this equation and its counterpart obtained by taking the cross product of both sides with $\mathbf{k}$ we obtain the dispersion relation (to avoid repetitiveness we skip the derivation details which can be found in (Kirkinis & Olvera de la Cruz 2023))

$$\omega = \pm\frac{\left[2\Omega + \nu_o(k_x^2 + k_y^2)\right]k_z}{k}, \quad \text{or} \quad \omega = \pm\left[2\Omega + \nu_o k^2\sin^2\theta\right]\cos\theta \tag{S4}$$

where $k = \sqrt{k_x^2 + k_y^2 + k_z^2}$ and in the latter equation θ is the angle between the $\mathbf{k}$ and the anisotropy/rotation z-axis. In Fig. S-IV we plot the dispersion ω (Eq. (S4)) versus angle θ. From the second of Eq. (S4) it is clear that the dispersion not only vanishes at $\theta = \pi/2$ as the case was for an inviscid fluid rotating with angular velocity Ω, but also

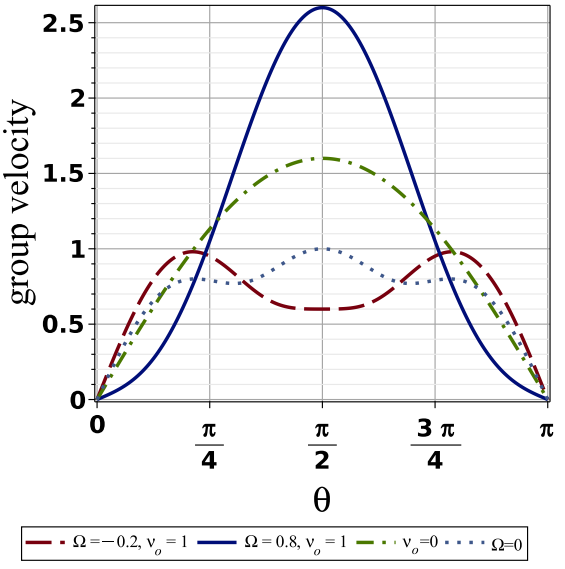

Figure S-V: Plane-polarized wave group velocity (S11) versus angle θ between the wavevector $\mathbf{k}$ and the z- (anisotropy) axis, setting $k = \nu_o = 1$ in arbitrary units. Of interest is the dashed curve denoting the existence of non-convex dispersion for the displayed parameters since the group velocity becomes maximum and the second derivative $|\partial^2_{k_i k_j}\omega|$ vanishes (cf. Fig. S-VI), implying the presence of caustics and a breakdown of the longtime asymptotics. The behavior denoted by the dashed line has implications on the helicity of the flow, since the maximum group velocity is found at a polar angle θ not equal to $\pi/2$ (which is the angle of maximum group velocity for a rigidly-rotating (not odd) liquid, cf. (Davidson 2013)).

vanishes when

$$\theta = \cos^{-1}\frac{\sqrt{\nu_o(k^2\nu_o + 2\Omega)}}{k\nu_o}, \tag{S5}$$

for suitable values of the parameters, as is apparent in Fig. S-IV (dashed line).

With the unit vector $\hat{\mathbf{k}} = \frac{\mathbf{k}}{k}$ in the direction of the wave-vector and the complex amplitude $\mathbf{A} = \mathbf{a} + i\mathbf{b}$ where $\mathbf{a}$ and $\mathbf{b}$ are real vectors, Eq. (S3) and the dispersion relation (S4) lead to $\hat{\mathbf{k}} \times \mathbf{b} = \mathbf{a}$, that is, the two vectors $\mathbf{a}$ and $\mathbf{b}$ are perpendicular to each other, are of the same magnitude and lie in the plane whose normal is $\mathbf{k}$. Thus, the velocity field is circularly polarized in the plane defined by $\mathbf{a}$ and $\mathbf{b}$ and is of the form

$$\mathbf{v} = \mathbf{a}\cos(\mathbf{k}\cdot\mathbf{r} - \omega t) - \mathbf{b}\sin(\mathbf{k}\cdot\mathbf{r} - \omega t), \quad \mathbf{a} \perp \mathbf{b}. \tag{S6}$$

Employing the negative sign of the dispersion relation (S4), the above analysis leads to the same velocity field (S6) but with the sense of the vectors $\mathbf{a}$ and $\mathbf{b}$ reversed: $\hat{\mathbf{k}}\times\mathbf{b} = -\mathbf{a}$.

It is of interest to calculate the group velocity. We obtain

$$\left(\frac{\partial\omega}{\partial k_x}, \frac{\partial\omega}{\partial k_y}\right) = \frac{k_z\left[\nu_o(k^2 + k_z^2) - 2\Omega\right]}{k^3}(k_x, k_y), \quad \frac{\partial\omega}{\partial k_z} = \frac{\left[2\Omega + \nu_o(k_x^2 + k_y^2)\right](k_x^2 + k_y^2)}{k^3}, \tag{S7}$$

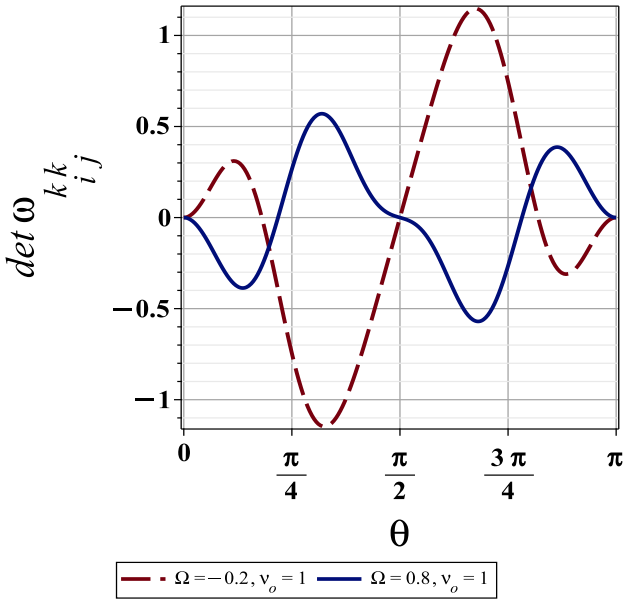

Figure S-VI: Determinant of the matrix $\omega_{k_i k_j} \equiv \partial^2_{k_i k_j}\omega$ in (S12) versus angle θ between the wavevector $\mathbf{k}$ and the z- (anisotropy) axis, setting $k = \nu_o = 1$ in arbitrary units. Of interest is the dashed curve for the indicating parameter values, which, for the negative values of Ω vanishes at angle $\theta = \cos^{-1}\sqrt{\frac{F}{5\nu_o k^2}}$ (cf. second line of Table S-II) corresponding to the inflexion points of the dispersion relation (cf. Fig. S-IV) and the extrema of the group velocity (cf. Fig. S-V), indicating the presence of caustics (overlapping of space-time rays (Ostrovsky & Potapov 1999, Fig. 6.3)). The vanishing of the positive Ω curve at $\theta = \cos^{-1}\sqrt{\frac{2\Omega - k^2\nu_o}{\nu_o k^2}}$ (cf. first line of Table S-II) does not correspond to maxima of the group velocity.

or, taking the z axis to be the axis of anisotropy we obtain

$$\left(\frac{\partial\omega}{\partial k_x}, \frac{\partial\omega}{\partial k_y}\right) = \sin\theta\cos\theta\frac{\nu_o k^2(1+\cos^2\theta) - 2\Omega}{k}(\cos\phi, \sin\phi), \tag{S8}$$

$$\frac{\partial\omega}{\partial k_z} = \frac{\nu_o k^2\sin^2\theta + 2\Omega}{k}\sin^2\theta. \tag{S9}$$

In contrast to the case of waves in a rotating fluid where the energy propagates perpendicularly to the wave-vector (along the axis of rotation) here the energy propagation direction has a component along the $\mathbf{k}$ axis:

$$\frac{\partial\omega}{\partial\mathbf{k}} = \nu_o k\left\{\hat{\mathbf{k}}(\hat{\mathbf{z}}\cdot\hat{\mathbf{k}})\left[1+(\hat{\mathbf{z}}\cdot\hat{\mathbf{k}})^2\right] + \hat{\mathbf{z}}\left[1-3(\hat{\mathbf{z}}\cdot\hat{\mathbf{k}})^2\right]\right\} + \frac{2\Omega}{k}\left[\hat{\mathbf{z}} - \hat{\mathbf{k}}(\hat{\mathbf{z}}\cdot\hat{\mathbf{k}})\right], \tag{S10}$$

thus the group velocity is not perpendicular to the phase velocity (direction of propagation) in contradistinction to the rigidly-rotating liquid case. The modulus of the group velocity is

$$\left|\frac{\partial\omega}{\partial\mathbf{k}}\right| = \frac{\sin\theta\sqrt{5\left(\cos^4\theta\right)k^4\nu_o^2 - 2k^2\nu_o\left(k^2\nu_o + 6\Omega\right)\left(\cos^2\theta\right) + \left(k^2\nu_o + 2\Omega\right)^2}}{k}. \tag{S11}$$

θ: root of Eq. (S12)	group velocity $\mathbf{c}_g$ evaluated at a root θ of Eq. (S12)
$\cos^{-1}\sqrt{\frac{2\Omega-k^2\nu_o}{\nu_o k^2}}$	$\frac{4(k^2\nu_o-\Omega)}{k}\hat{\mathbf{z}}$
$\cos^{-1}\sqrt{\frac{F}{5\nu_o k^2}}$	$\frac{\sqrt{F(5\nu_o k^2-F)}(5\nu_o k^2+F-10\Omega)}{25\nu_o k^3}(\cos\phi\hat{\mathbf{x}}+\sin\phi\hat{\mathbf{y}})+\frac{(F-5\nu_o k^2-10\Omega)(F-5\nu_o k^2)}{25\nu_o k^3}\hat{\mathbf{z}}$
$\frac{\pi}{2}$	$\frac{k^2\nu_o+2\Omega}{k}\hat{\mathbf{z}}$

Table S-II: Summary of functional expressions attained by group velocity at its extrema determined by the roots of Eq. (S12). The group velocity thus has extrema that differ from the known cases of zero rotation or zero odd viscosity, displayed in the third line.

In Fig. S-V we plot the group velocity magnitude (S11) versus angle θ (formed between the wavevector $\mathbf{k}$ and the z- (rotation) axis, setting $k=\nu_o=1$).

The determinant of the second derivative of the dispersion relation $\partial^2_{k_ik_j}\omega$ becomes

$$|\partial^2_{k_ik_j}\omega| = \frac{1}{k^6}\cos\theta\sin^2\theta\left(5k^4\nu_o^2\cos^4\theta-4\nu_o k^2\left(k^2\nu_o+4\Omega\right)\cos^2\theta-\left(k^2\nu_o-2\Omega\right)^2\right) \times\left(k^2\nu_o\cos^2\theta+k^2\nu_o-2\Omega\right) \tag{S12}$$

The extrema of the group velocity related to the roots of $|\partial^2_{k_ik_j}\omega|$ are displayed in Table S-II. In its third line we recognize the group velocity $\frac{k^2\nu_o+2\Omega}{k}\hat{\mathbf{z}}$ with energy propagating along the axis of rotation/anisotropy known from the literature (Davidson 2013; Kirkinis & Olvera de la Cruz 2023) when the wavevector is perpendicular to this axis ($\theta=\pi/2$). From the first and second lines of the Table we however see that depending on the parameter values and signs for odd viscosity ν_0 and angular velocity Ω there might be different wavenumber directions ($\theta\neq\pi/2$) with the energy propagating along the axis or at an angle to it.

S-IV.2. *Effects of both η_o and η_4 odd viscous stresses*

Apart from Eq. (S1), there is also a second odd viscous (non-dissipative) constitutive law that may be employed to describe the properties of an odd viscous liquid (Lifshitz & Pitaevskii 1981, §58)

$$\boldsymbol{\sigma}' = \eta_4\begin{pmatrix} 0 & 0 & -(\frac{1}{r}\partial_\phi v_z+\partial_z v_\phi)\\ 0 & 0 & \partial_r v_z+\partial_z v_r\\ -(\frac{1}{r}\partial_\phi v_z+\partial_z v_\phi) & \partial_r v_z+\partial_z v_r & 0\end{pmatrix}. \tag{S13}$$

Although combination of the two constitutive laws (S1) and (S13) with rigid-rotation of angular velocity Ω is complicated, its consequences on fluid-flow behavior can be obtained by performing the substitution

$$\nu_o\to\nu_o-\nu_4,\quad\text{and}\quad 2\Omega\to 2\Omega+\nu_4k^2 \tag{S14}$$

in the results already obtained in section S-I. This can be seen, for instance, from the reduced form of Eq. (S8)

$$-i\omega v_r = -i\frac{\omega}{k^2}\mathcal{L}v_r-\left[(\nu_o-\nu_4)\mathcal{L}-2\Omega-\nu_4k^2\right]v_\phi, \tag{S15}$$

$$-i\omega v_\phi = \left[(\nu_o-\nu_4)\mathcal{L}-2\Omega-\nu_4k^2\right]v_r \tag{S16}$$

and this is exactly the form of the Navier-Stokes equations when constitutive laws (S1) and (S13) are jointly employed. Thus, considering velocity fields $v_r, v_\phi\propto J_1(\kappa r)$ as in

section S-I, we obtain exactly the same type of κ roots as those described in Fig. S-II and Table S-I by making the substitution (S14). We thus do not need to discuss this case further.

For plane polarized waves one can perform the substitution (S14) and obtain the same results as in section S-IV.1 with the exception of the group velocity and higher order derivatives of ω with respect to k_z. We briefly discuss the governing equations since they can be expressed in a concise form and lead to certain conclusions about the helicity of the flow. Another reason for wanting to discuss both odd viscosity coefficients ν_o and ν_4 is that certain combinations have been employed in the literature to simplify the discussion cf. (Markovich & Lubensky 2021; Khain *et al.* 2022) and in particular the combination $\eta_o = 2\eta_4$ which we call elliptic. Also the (parabolic) combination $\eta_o = \eta_4$ simplifies the discussion significantly. The names elliptic or parabolic are inherited from the form obtained by the governing differential operator $\mathcal{S}$ that will be defined below.

Expressing both odd stress tensors (S1) and (S13) in Cartesian coordinates we obtain

$$\boldsymbol{\sigma}' = \begin{pmatrix} -\eta_o\left(\partial_x v + \partial_y u\right) & \eta_o(\partial_x u - \partial_y v) & -\eta_4(\partial_y w + \partial_z v) \\ \eta_o(\partial_x u - \partial_y v) & \eta_o(\partial_x v + \partial_y u) & \eta_4(\partial_x w + \partial_z u) \\ -\eta_4(\partial_y w + \partial_z v) & \eta_4(\partial_x w + \partial_z u) & 0 \end{pmatrix}. \tag{S17}$$

Let

$$\mathcal{S} = (\nu_o - \nu_4)\nabla_2^2 + \nu_4\partial_z^2 \quad \text{or equivalently,} \quad \mathcal{S} = (\nu_o - \nu_4)\nabla^2 + (2\nu_4 - \nu_o)\partial_z^2. \tag{S18}$$

With $\zeta = \partial_x v - \partial_y u$ denoting the component of vorticity in the z direction and a modified pressure $\tilde{p} = p + \eta_4\zeta$, the Navier-Stokes equations of a rigidly-rotating liquid, characterized by the constitutive law (S17), become

$$\frac{D\mathbf{v}}{Dt} = -\frac{1}{\rho}\nabla\tilde{p} + (\mathcal{S} - 2\Omega)\hat{\mathbf{z}} \times \mathbf{v}. \tag{S19}$$

The linearized vorticity equation (S1) is thus replaced by

$$\partial_t \mathrm{curl}\mathbf{v} = -(\mathcal{S} - 2\Omega)\frac{\partial \mathbf{v}}{\partial z}. \tag{S20}$$

With $\mathbf{v} = \mathbf{A}e^{i(\mathbf{k}\cdot\mathbf{r} - \omega t)}$, the dispersion relation becomes

$$\omega = \pm\left[2\Omega - \mathcal{S}(\mathbf{k})\right]\frac{k_z}{k} \quad \text{or} \quad \omega = \pm\cos\theta\left\{k^2\left[\nu_o - \nu_4 - (\nu_o - 2\nu_4)\cos^2\theta\right] + 2\Omega\right\} \tag{S21}$$

where $k = \sqrt{k_x^2 + k_y^2 + k_z^2}$ and

$$\mathcal{S}(\mathbf{k}) = -(\nu_o - \nu_4)(k_x^2 + k_y^2) - \nu_4 k_z^2 \quad \text{or} \quad \mathcal{S}(\mathbf{k}) = -(\nu_o - \nu_4)k^2 - (2\nu_4 - \nu_o)k_z^2. \tag{S22}$$

The group velocity becomes

$$\left(\frac{\partial\omega}{\partial k_x}, \frac{\partial\omega}{\partial k_y}\right) = \pm\left[k\left((\nu_o - 2\nu_4)\cos^2\theta + \nu_o - \nu_4\right) + 2\Omega\right]\sin\theta\cos\theta(\cos\phi, \sin\phi), \tag{S23}$$

$$\frac{\partial\omega}{\partial k_z} = \pm k\left((\nu_o - 2\nu_4)\cos^4\theta + (-2\nu_o + 5\nu_4)\cos^2\theta + \nu_o - \nu_4\right) \pm 2\Omega. \tag{S24}$$

As can be seen, the above relations simplify significantly in the limits $\nu_o = 2\nu_4$ or $\nu_o = \nu_4$. The former recovers Eq. (8) of Markovich & Lubensky (2021),

$$\omega = \nu_4 k k_z + 2\Omega\frac{k_z}{k}, \tag{S25}$$

now for an odd viscous liquid rotating rigidly with angular velocity Ω.

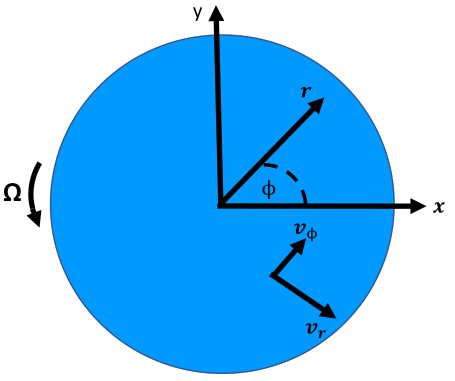

Figure S-VII: Two-dimensional odd viscous compressible liquid rotating with angular velocity Ω. In plane polar coordinates the velocity field is $\mathbf{v} = v_r\hat{\mathbf{r}} + v_\phi\hat{\boldsymbol{\phi}}$ in the frame rotating with the liquid at constant angular velocity Ω.

Helicity is conserved for an odd viscous liquid that incorporates the constitutive law (S17). We show this by considering the linearized vorticity equation (S20) written in the form

$$-i\omega\mathbf{B} = i\mathbf{A}k_z\left[2\Omega - \mathcal{S}(\mathbf{k})\right], \tag{S26}$$

when $\mathrm{curl}\mathbf{v} = \mathbf{B}e^{i(\mathbf{k}\cdot\mathbf{r}-\omega t)}$ and $\mathcal{S}(\mathbf{k})$ is defined in Eq. (S22). Since $\omega = \pm\left[2\Omega - \mathcal{S}(\mathbf{k})\right]\frac{k_z}{k}$ (from (S21)) we obtain $\mathbf{B} = \mp k\mathbf{A}$, or

$$\mathrm{curl}\mathbf{v} = \mp k\mathbf{v}. \tag{S27}$$

Thus, the helicity of the flow field determined by the odd stress tensor (S17) is conserved

$$\mathbf{v}\cdot\mathrm{curl}\mathbf{v} = \mp k|\mathbf{v}|^2 \tag{S28}$$

which can be seen from the form of the velocity field (S6) for $\mathbf{a}\perp\mathbf{b}$.

S-V. Inertial oscillations in a rigidly-rotating compressible two-dimensional odd viscous liquid

S-V.1. *Axisymmetric inertial-like waves*

A two dimensional compressible liquid endowed with odd viscosity obeys the constitutive law (Lapa & Hughes 2014; Ganeshan & Abanov 2017)

$$\boldsymbol{\sigma}' = \eta_o\begin{pmatrix} -\left(\partial_r v_\phi - \frac{1}{r}v_\phi + \frac{1}{r}\partial_\phi v_r\right) & \partial_r v_r - \frac{1}{r}v_r - \frac{1}{r}\partial_\phi v_\phi \\ \partial_r v_r - \frac{1}{r}v_r - \frac{1}{r}\partial_\phi v_\phi & \partial_r v_\phi - \frac{1}{r}v_\phi + \frac{1}{r}\partial_\phi v_r \end{pmatrix}, \tag{S1}$$

and the continuity equation

$$\partial_t\rho' + \rho\mathrm{div}\mathbf{v} = 0 \quad \text{for} \quad \rho' \ll \rho, \tag{S2}$$

where ρ' is the variable part of the density and ρ a constant background level. As in section S-I, consider an axisymmetric geometry, now described by plane polar coordinates r, ϕ (cf. Fig. S-VII) the fields are independent of ϕ, we neglect nonlinear terms (assuming small-amplitude motions) and the time dependence is given by the factor $\exp[-i\omega t]$ where ω is a real frequency. Employing the constitutive law (S1), the linearized equations of motion become (Lifshitz & Pitaevskii 1981, §89)

$$-i\omega v_r = -\frac{c^2}{\rho}\frac{\partial \rho'}{\partial r} + 2\Omega v_\phi - \nu_o\left[\frac{1}{r}\frac{\partial}{\partial r}\left(r\frac{\partial v_\phi}{\partial r}\right) - \frac{v_\phi}{r^2}\right], \tag{S3}$$

$$-i\omega v_\phi = -2\Omega v_r + \nu_o\left[\frac{1}{r}\frac{\partial}{\partial r}\left(r\frac{\partial v_r}{\partial r}\right) - \frac{v_r}{r^2}\right], \tag{S4}$$

$$-i\omega \rho' = -\rho\frac{1}{r}\frac{\partial}{\partial r}\left(r v_r\right), \tag{S5}$$

where c is the speed of sound. Because of Eq. (S5) we obtain

$$\frac{\partial \rho'}{\partial r} = \frac{\rho}{i\omega}\frac{\partial}{\partial r}\left(\frac{1}{r}\frac{\partial}{\partial r}\left(r v_r\right)\right). \tag{S6}$$

We again employ the identity $\frac{\partial}{\partial r}\left(\frac{1}{r}\frac{\partial}{\partial r}\left(r v_r\right)\right) = \frac{1}{r}\frac{\partial}{\partial r}\left(r\frac{\partial v_r}{\partial r}\right) - \frac{v_r}{r^2}$, and the linear operator $\mathcal{L} = \partial_r^2 + \frac{1}{r}\partial_r - \frac{1}{r^2}$ we introduced in Eq. (S7). The r and ϕ momentum equations (S3), (S4) become

$$-i\omega v_r = -\frac{c^2}{i\omega}\mathcal{L}v_r - (\nu_o\mathcal{L} - 2\Omega)v_\phi, \tag{S7}$$

$$-i\omega v_\phi = (\nu_o\mathcal{L} - 2\Omega)v_r. \tag{S8}$$

Expressing the velocities v_r and v_ϕ in terms of Bessel or modified Bessel functions, $v_r = AJ_1(\kappa r), v_\phi = BJ_1(\kappa r)$, or $v_r = AI_1(\kappa r), v_\phi = BI_1(\kappa r)$, etc., (where A and B are constants to be determined by the boundary conditions and κ is an eigenvalue) the system (S7) and (S8) has a solution when the determinant $-\kappa^4\nu_o^2 - 4\Omega\,\kappa^2\nu_o - c^2\kappa^2 - 4\Omega^2 + \omega^2$ of the coefficients of the resulting linear system

$$-\frac{i\left(-\kappa^2\nu_o - 2\Omega\right)B\omega - A\,c^2\kappa^2}{\omega^2} - A = 0, \quad \text{and} \quad \frac{iA\left(-\kappa^2\nu_o - 2\Omega\right)}{\omega} - B = 0 \tag{S9}$$

vanishes. Consider first the case where the origin is included in the domain. It is not difficult to show that the solution is the Bessel function $J_1(\kappa r)$ for which κ satisfies

$$\kappa^2 = \frac{-4\Omega\nu_o - c^2 + \sqrt{8\Omega\,c^2\nu_o + c^4 + 4\nu_o^2\omega^2}}{2\nu_o^2}. \tag{S10}$$

As with Eq. (S12) of the three-dimensional case of section S-I, Eq. (S10) here is a relation between the allowed (possibly complex) eigenvalue κ and the (real) frequency ω. We can cast Eq. (S10) in a form resembling (S12) and (S14). Thus,

$$\nu_o\kappa^2 = -\frac{c^2}{2\nu_o} - 2\Omega \pm \sqrt{\left(-\frac{c^2}{2\nu_o} - 2\Omega\right)^2 + \omega^2 - (2\Omega)^2} \equiv \alpha \pm \sqrt{\alpha^2 + \beta} \tag{S11}$$

where we carried-out the substitution

$$\alpha = -\frac{c^2}{2\nu_o} - 2\Omega, \quad \beta = \omega^2 - (2\Omega)^2, \tag{S12}$$

to be compared with the definition of α and β in (S13). Therefore the classification of the roots κ of Eq. (S12) displayed in, Fig. S-II and Table S-I, carry-over in the present section unchanged by making the substitution (S12). We display the parameter regimes again in Fig. S12 with respect to the new meaning of the parameter α.

Thus, overall we found that inertial-like waves in a compressible two dimensional and rigidly rotating odd viscous liquid exist and have the velocity fields and density

$$v_r = AJ_1(\kappa r)e^{-i\omega t}, \quad v_\phi = -iA\frac{2\Omega + \nu_o\kappa^2}{\omega}J_1(\kappa r)e^{-i\omega t}, \quad \rho' = -iA\frac{\rho\kappa}{\omega}J_0(\kappa r)e^{-i\omega t} \tag{S13}$$

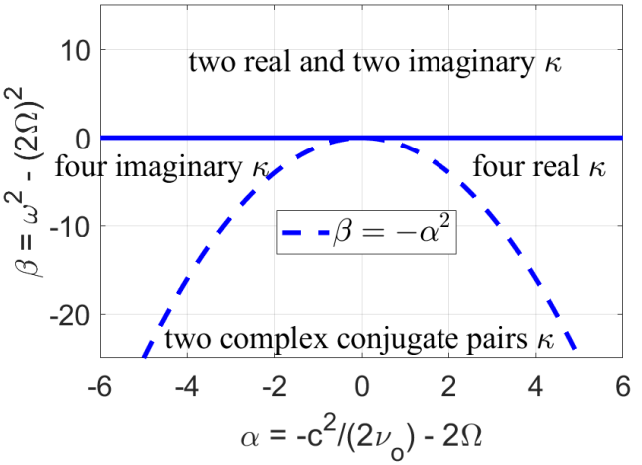

Figure S-VIII: Roots of Eq. (S10) in the parameter space (α, β) defined in Eq. (S12). Rich behavior exists in the presence of rotation. This includes the oscillatory Bessel functions for real κ, exponentially increasing/decreasing Bessel functions for κ imaginary and exponential-oscillating Bessel functions for complex κ (see Fig. S-II for the qualitative form of these Bessel functions)

and these resemble their three-dimensional counterparts of Eq. (S15).

S-VI. Illustrative examples

S-VI.1. *Inertial oscillations of a two-dimensional odd viscous liquid in a disk*

Consider the case where $\omega \sim 2\Omega$ and thus $\nu_o\kappa^2 \sim 2\alpha = 2\left(-\frac{c^2}{2\nu_o} - 2\Omega\right)$ or $\nu_o\kappa^2 = 0$ from Eq. (S11). Two real roots exist as long as $4\Omega < -c^2/\nu_o$ and the velocity field is given by (S13). This motion comprises regions between concentric circles of radius r_n such that

$$r_n\kappa = \gamma_n \tag{S1}$$

and γ_n are the zeros of $J_1(x)$. Both v_r and v_ϕ vanish at these concentric circles and the fluid does not cross them. Introducing the polar form for the amplitude $A = ae^{i\theta}$, where a and θ are real amplitude and phase, we can cast the complex fields of (S13) in real form

$$v_r = aJ_1(\kappa r)\cos(\theta - \omega t), \quad v_\phi = a\frac{2\Omega + \nu_o\kappa^2}{\omega}J_1(\kappa r)\sin(\theta - \omega t), \quad \rho' = a\frac{\rho\kappa}{\omega}J_0(\kappa r)\sin(\theta - \omega t). \tag{S2}$$

We consider the liquid confined within a solid cylindrical surface located, say, at $r = b$, that would be realistic in a laboratory setting. This boundary will be a streamline located at an integral number of cells in the radial direction. If by γ_n we denote the n-th zero of the Bessel function J_1, Eq. (S11) with the condition $\kappa b = \gamma_n$ lead to the constraint

$$b\left(\frac{-4\Omega\nu_o - c^2 + \sqrt{8\Omega\, c^2\nu_o + c^4 + 4\nu_o^2\omega^2}}{2\nu_o^2}\right)^{1/2} = \gamma_n \tag{S3}$$

and n denotes the number of cells in the radial direction (cf. Fig. S-III). From Eq. (S3)

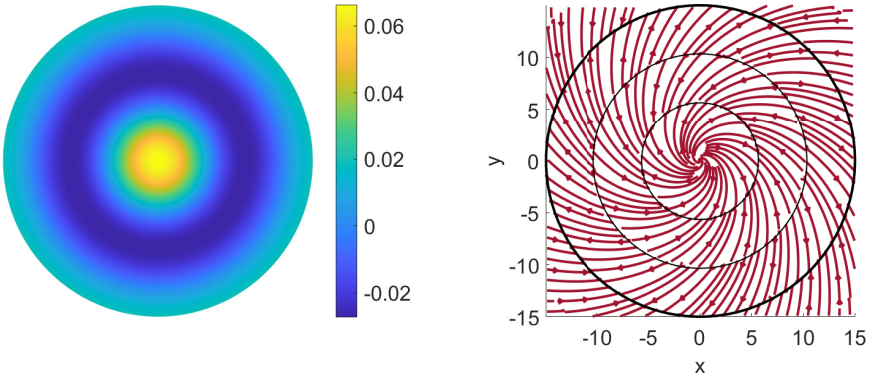

Figure S-IX: **Left panel**: Colorbar: density ρ' (arbitrary units) in (S2) for a two-dimensional compressible odd viscous liquid contained in a disk of radius $b = \gamma_3/\kappa$ where $\gamma_3 = 10.173$ is the third zero of the Bessel function J_1. **Right panel**: Instantaneous streamlines in the $x - y$ plane (measured in arbitrary units) of the velocity field v_r and v_ϕ in (S2) , representing oscillations of an odd viscous liquid with frequency ω. The liquid is contained in the disk denoted by the thick black circle. The two interior thin black circles have been included only as a guide to the eye and denote the location of the zeros of the Bessel function J_1, that is, the location where the velocity vanishes. For a liquid that extends beyond the disk, its streamlines are as shown in the region outside the thick black circle.

one can relate the frequency of oscillation ω with the cylinder radius b

$$\omega^2 = (\nu_o \kappa^2 + 2\Omega)^2 + (c\kappa)^2, \quad \kappa = \frac{\gamma_n}{b}, \tag{S4}$$

where n denotes the number of cells in the radial direction.

In Fig. S-IX we plot the density ρ' in (S2) when the liquid is contained in a disk of radius $b = \gamma_3/\kappa$ where $\gamma_3 = 10.173$ is the third zero of the Bessel function J_1 and the corresponding instantaneous streamlines of the velocity field v_r and v_ϕ in (S2). The streamlines contained between two adjacent concentric circles change direction periodically with period $T = 2\pi/\omega$.

S-VI.2. *Polarized waves*

When the wavenumber κ in (S4) is real one can develop the counterpart of the three-dimensional plane polarized waves of section S-IV. The important point is that for certain parameter regimes the dispersion relation (S4) can become non-convex. At an inflection point of the dispersion relation (S4) the group velocity is maximum and the determinant of $\partial_{k_i}\partial_{k_j}\omega$ vanishes. This implies that rays (characteristics) of the nonlinear transport equation $\partial_t\omega + \mathbf{c}_g(\omega)\cdot\nabla\omega = 0$ carrying an initial frequency profile, overlap at a specific interval of space and time giving rise to a caustic curve (Lighthill 1978; Ostrovsky & Potapov 1999). Although this behavior is still physically realistic, the ray theory (where slow variations of wavenumber are assumed) employed to calculate Fourier integrals in wavenumber space breaks down; the method of stationary needs to be modified by employing higher order derivatives of ω with respect to $\mathbf{k}$ (usually third order derivatives) in these Fourier integrals. When nonlinear terms are added to these linear systems, unusual behavior is observed such as oscillatory soliton tails and dispersive shocks (Lowman & Hoefer 2013; Sprenger & Hoefer 2017) arising as radiation

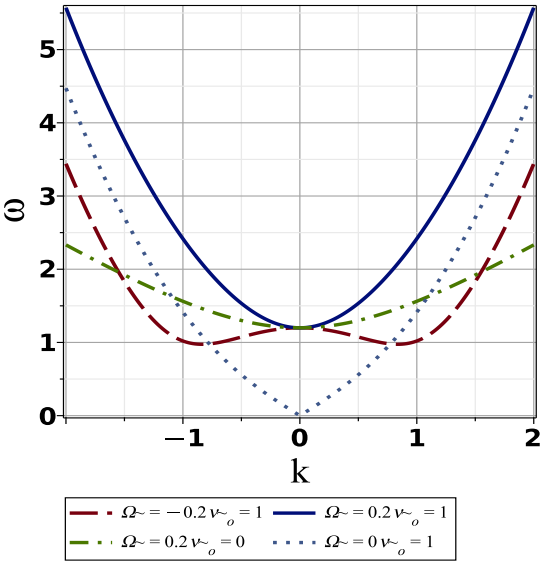

Figure S-X: Dispersion relation (S6) versus wavenumber $k = k_x$ (evaluated at $k_y = 0$ for clarity and measured in arbitrary units). Of primary interest is the dashed curve denoting the existence of non-convex dispersion for the displayed parameters ($\Omega\nu_o < 0$). At its inflection points the corresponding group velocity attains its maximum value (cf. Fig. S-XI) and the second derivative $|\partial^2_{k_i k_j}\omega|$ vanishes (cf. Fig. S-XII), implying the presence of caustics and a breakdown of the longtime asymptotics. The dotted line ($\Omega = 0, \nu_o \neq 0$) is also of interest since the dispersion curve develops a cusp at $k = 0$. Thus, the group velocity develops a jump as one traverses k_x from negative to positive values (cf. Fig. S-XI).

due to motion of the medium emanating when the velocity of particles moving in it is larger than the phase velocity of waves that propagate in this medium (Cherenkov radiation, cf, (Landau & Lifshitz 1960; Kuznetsov & Dias 2011)). Here we will not pause to display these nonlinear effects, most of which are well-known in the literature. We will establish the existence of planar inertial-like waves and discuss the behavior of the dispersion that may give rise to the aforementioned effects.

Let $\psi = k_1 v_2 - k_2 v_1$ and $\chi = k_1 v_1 + k_2 v_2$ where v_i are the velocity components of a two-dimensional compressible odd viscous liquid in Cartesian coordinates. Thus, $\psi = \mathrm{curl}\mathbf{v}^t$ and $\chi = \mathrm{div}\mathbf{v}^l$ (in coordinate space), are the derivatives of the transverse and longitudinal velocity components, respectively. Then, we can replace the balance of linear momentum with two equations for χ and ψ (see for instance (Landau & Lifshitz 1980, §89))

$$\frac{d\chi}{dt} = -ik^2c^2\frac{\rho'}{\rho} + (2\Omega + \nu_o k^2)\psi, \quad \frac{d\psi}{dt} = -(2\Omega + \nu_o k^2)\chi, \quad \frac{d\rho'}{dt} = -i\rho\chi \tag{S5}$$

where we employed the notation χ, ρ and ψ to denote quantities in both coordinate and momentum representation. We can derive a single second order linear oscillator equation for χ, namely $\frac{d^2\chi}{dt^2} + \omega^2\chi = 0$, where

$$\omega^2 = (kc)^2 + (2\Omega + \nu_o k^2)^2, \quad \text{for} \quad k = \sqrt{k_x^2 + k_y^2}. \tag{S6}$$

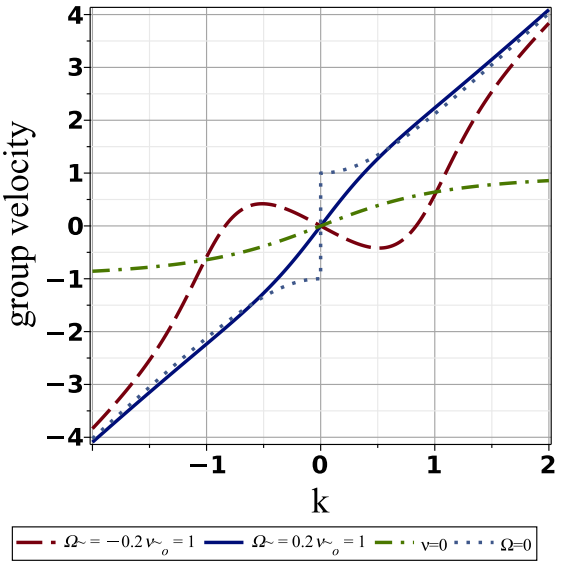

Figure S-XI: $k = k_x$ component of the group velocity (S7) (setting $k_y = 0$ for clarity and measured in arbitrary units). Of interest is the dashed curve for the indicating parameter values, which attains local maxima and minima corresponding to the inflexion points of the dispersion relation (cf. Fig. S-X) and the vanishing of the determinant second derivative $|\partial^2_{k_i k_j}\omega|$ (cf. Fig. S-XII), indicating the presence of caustics (overlapping of space-time rays (Ostrovsky & Potapov 1999, Fig. 6.3)). Of interest is also the dotted line (odd viscosity in the absence of rotation) which displays a jump at $k = 0$.

The group velocity associated with dispersion (S4) becomes

$$\mathbf{c}_g = \frac{\left(2k^2\nu_o^2 + \tilde{c}^2\right)}{\sqrt{k^4\nu_o^2 + \tilde{c}^2k^2 + 4\Omega^2}}(k_x, k_y) \tag{S7}$$

where $\tilde{c}^2 = 4\Omega\nu_o + c^2$ whose significance will be discussed in section S-VI.3, and the determinant of the matrix $\partial^2_{k_i k_j}\omega$ is

$$|\partial^2_{k_i k_j}\omega| = \frac{\left[2k^2\nu_o^2(\nu_o^2k^4 + 12\Omega^2) + \tilde{c}^2(3\nu_o^2k^4 + 4\Omega^2)\right]\left(2k^2\nu_o^2 + \tilde{c}^2\right)}{\left(k^4\nu_o^2 + \tilde{c}^2k^2 + 4\Omega^2\right)^2}, \tag{S8}$$

and comparison of (S7) with (S8) shows that they share a common zero.

With respect to the dashed curve in Figures S-X-S-XII, representing the dispersion, group velocity and second derivative of dispersion of a rigidly-rotating odd viscous liquid with $\Omega\nu_o < 0$ we point-out the following characteristics.

(i) At the inflection point of the dispersion curve (S6) the group velocity is maximum and $|\partial^2_{k_i k_j}\omega|$ vanishes.

(ii) At the bottom of the well (the minimum of the dispersion curve) in (S6) the group velocity vanishes and $|\partial^2_{k_i k_j}\omega|$ vanishes as well.

With respect to the dotted curve in Figures S-X-S-XI, representing the dispersion and group velocity of a rigidly-rotating odd viscous liquid with $\Omega \equiv 0$ we point-out the following characteristics.

(i) The dispersion curve (S6) has a cusp at $k = 0$, $\omega \sim c|k|$.

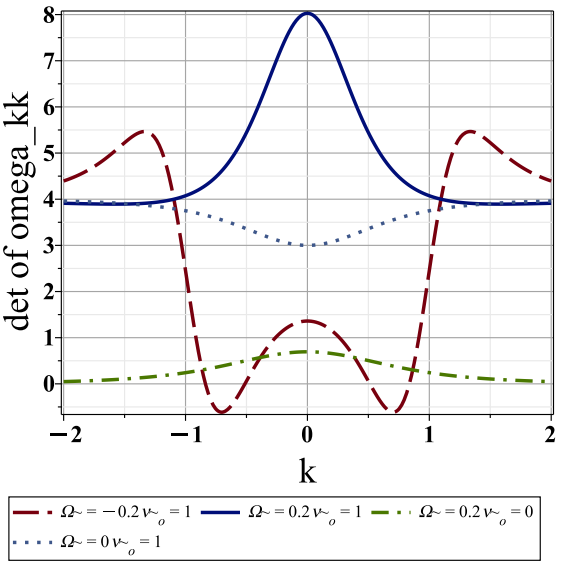

Figure S-XII: Determinant of the matrix $\partial^2_{k_i k_j}\omega$ in (S8) vs. $k = k_x$ (setting $k_y = 0$ for compatibility with the two previous figures and measured in arbitrary units). Of interest is the dashed curve for the indicating parameter values, which vanishes near $k_x \sim \pm 0.5$ corresponding to the inflexion points of the dispersion relation (cf. Fig. S-X) and the extrema of the group velocity (cf. Fig. S-XI), indicating the presence of caustics (overlapping of space-time rays (Ostrovsky & Potapov 1999, Fig. 6.3)).

(ii) The group velocity is equal to $\mp c$, as we approach the $k = 0$ line from the left (negative sign) and the right (positive sign).

The determinant $|\partial^2_{k_i k_j}\omega|$ in (S8) vanishes at two locations as indicated in Fig. S-XII. First, at the zero $k^2 = \frac{4\Omega\nu_o + c^2}{-2\nu_o^2}$ it shares with the group velocity, and second at

$$k^2 = \frac{\left(4c^{\frac{2}{3}}\,\Omega\nu_o + c^{\frac{8}{3}}\right)\left(8\Omega\nu_o + c^2\right)^{\frac{2}{3}} + c^4 + 8\Omega c^2\nu_o + c^{\frac{4}{3}}\left(8\Omega\nu_o + c^2\right)^{\frac{4}{3}}}{-2\left(8\Omega\nu_o + c^2\right)^{\frac{2}{3}}\,c^{\frac{2}{3}}\nu_o^2}. \tag{S9}$$

Only specific values of the parameters give rise to real observables in these relations.

S-VI.3. *Topologically protected waves*

The analysis of section S-V.1 can be applied to describe *qualitatively* the behaviour of density waves that do not scatter off an obstacle and propagate unidirectionally, (refered to here as cases I & II, displayed in Table S-III) studied numerically in (Souslov *et al.* 2019, Eq. (3)).

In (Souslov *et al.* 2019) three parameter regimes are chosen to demonstrate three distinct behaviours, the first two giving rise to unidirectional wave propagation along the circular boundary and *no scattering* off a single obstacle. We tabulate the material parameters of these two cases in Table S-III. In case I, the first set of values $(c, \Omega, \nu_o, \rho) = (8, -20, 0.1, 1)$ gives in our parametric representation introduced in Eq. (S12)

$$(\alpha, \alpha^2 + \beta) = (-280, \omega^2 + 76800), \tag{S10}$$

which implies that equationn (S11) has four imaginary roots κ, by looking at the diagram in Fig. S-VIII (for $\omega \equiv 0$ these are $\kappa \sim \pm 5.36i, \pm 74.64i$). Thus, the exponentially

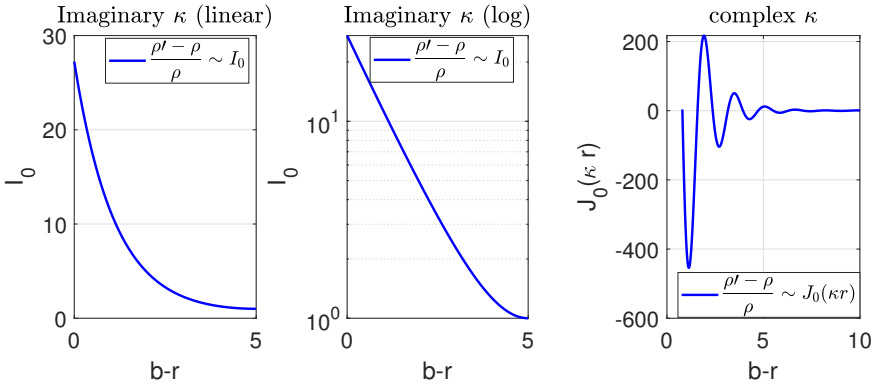

Figure S-XIII: Theoretical qualitative predictions of the model (S3)-(S5) for the behavior of the density ρ' in (S2) of a compressible odd viscous liquid in a disk. Left two panels (Case I of Table S-III): Density for imaginary κ, displayed in linear and logarithmic vertical axes respectively, obtained as solution of Eq. (S11). The horizontal axis denotes distance from a circular boundary located at $r = b$. When κ is complex, the rightmost panel (Case II of Table S-III) gives the characteristic behavior of the density. These profiles are to be compared with the numerical results of (Souslov *et al.* 2019) displayed in their Fig. 3(b) and 3(d). Thus, the density profile resembles an evanescent wave (see discussion at the end of section S-VI.3).

	c	Ω	ν_o	ρ	α	$\alpha^2+\beta$	Effect	Renormalized c
Case I	8	-20	0.1	1	-280	$\omega^2+76800$	no scattering	$\tilde{c}_I = 7.48$
Case II	15	-500	2	1	$3775/4$	$\omega^2-1749375/16$	no scattering	
Case III	8	20	0.1	1	-360	$\omega^2+128000$	scattering	$\tilde{c}_{III} = 8.48$

Table S-III: Parameter values (c, Ω, ν_o, ρ) employed in (Souslov *et al.* 2019) to numerically demonstrate the existence of topological waves. α and β are the parameters defined in Eq. (S12) to classify the system behaviours displayed in Fig. S-VIII. Parameter Cases I & II above leading to radial Navier-Stokes eigenvalues κ obtained as roots of Eq. (S10), are displayed in the left and right panel of Fig. 4 in the main manuscript, respectively, for arbitrary value of the frequency ω. Odd viscosity coupled to rigid rotation renormalizes the speed of sound of the medium and leads disturbances to propagate with supersonic (no scattering from a solid obstacle) or subsonic (scattered from a solid obstacle) speed, cf. Fig. S-XIV.

increasing (from the origin of the disk) solution representing the density ρ' of the liquid will have, in the radial direction, the form of the modified Bessel function I_0 (see Supplemental Material for the form of the density). We display in the left two panels of Fig. S-XIII the modified Bessel function I_0 in linear and logarithmic vertical axes, as a function of the radial coordinate $b - r$, that is, measuring distance from a boundary located at $r = b$. These two panels qualitatively capture the two graphs of Figure 3(b) in (Souslov *et al.* 2019) giving rise to the protected density waves of Fig. 3(a) of the same reference.

We repeat the above analysis for the second set of parameters employed in the analysis of (Souslov *et al.* 2019) $(c, \Omega, \nu_o, \rho) = (15, -500, 2, 1)$, since there is some interesting qualitative behaviour that can also be captured by our analysis. The parametric space

implied by Fig. S-VIII becomes in this case

$$(\alpha, \alpha^2 + \beta) = (3775/4, \omega^2 - 1749375/16). \tag{S11}$$

It can be seen from Eq. (S11) that the four κ's can be two complex conjugate pairs, all real or two real and two imaginary. For small $\omega \sim 0$ (as was considered in (Souslov *et al.* 2019)) we obtain two complex conjugate pairs (for $\omega \equiv 0$ these are $\kappa = \pm 5\sqrt{151 \pm 3i\sqrt{311}}/2$). Now the density ρ' of the liquid will have, in the radial direction, the form of the Bessel function $J_0(\kappa r)$ for complex κ. We display in the rightmost panel of Fig. Fig. S-XIII its real part as a function of the radial coordinate $b - r$, that is, measuring distance from a boundary located at $r = b$. Although the density is restricted by an exponentially decaying envelope, it also oscillates (characteristic behaviour of the Kelvin functions). Thus, the right-most panel of Fig. Fig. S-XIII qualitatively captures Figure 3(d) in (Souslov *et al.* 2019) giving rise to the protected density waves of Fig. 3(b) of the same reference. This oscillatory behaviour is most visible in the video provided by (Souslov *et al.* 2019).

The behaviours outlined above are displayed in Fig. 4 of the main manuscript for the real frequency ω vs. the real and imaginary parts of κ, drawn from (S11). See the discussion in the main manuscript.

There is also a third case of material parameters considered in (Souslov *et al.* 2019) where $\Omega\nu_o > 0$ (note that although the dispersion curve becomes non-convex when $\Omega\nu_o < 0$ and k_x, k_y are real in Eq. (S6), here the wavenumber is imaginary and the significance of the sign of $\nu_o\Omega$ reverses since now $\omega^2 = (-\nu_o\tilde{\kappa}^2 + 2\Omega)^2 - c^2\tilde{\kappa}^2$ for $\kappa = i\tilde{\kappa}$ with $\tilde{\kappa}$ being a real number). We tabulate the material parameters in Table S-III. Thus, in case III, the set of values $(c, \Omega, \nu_o, \rho) = (8, 20, 0.1, 1)$ gives in our parametric representation

$$(\alpha, \alpha^2 + \beta) = (-280, \omega^2 + 128000), \tag{S12}$$

which implies that equations (S10) or (S11) have four imaginary roots κ, by looking at the diagram in Fig. S-VIII (for $\omega \equiv 0$ these are $\kappa \sim \pm 4.72i, \pm 84.72i$). Thus, the exponentially increasing (from the origin of the disk) solution representing the density ρ' of the liquid will have, in the radial direction, the form of the modified Bessel function I_0.

There are however, qualitative differences between case I and case III. In case I one visually determines waves that do not scatter off from an obstacle, while in case III the waves do scatter (Souslov *et al.* 2019, SI-movie). We thus proceed to provide an alternative explanation to the topological numbers argument of (Souslov *et al.* 2019) for the above behaviour. Rewrite the dispersion relation in the form

$$\omega^2 = \nu_o^2\tilde{\kappa}^4 - \left[4\nu_o\Omega + c^2\right]\tilde{\kappa}^2 + 4\Omega^2, \tag{S13}$$

where, for cases I & III, we've set $\kappa = i\tilde{\kappa}$, $\tilde{\kappa}$ being a real number. The speed of sound in the medium has been renormalized by the product of odd viscosity with angular velocity Ω. Thus, let

$$\tilde{c} = \sqrt{4\nu_o\Omega + c^2}, \tag{S14}$$

be the renormalized speed of sound. Using the parameter values of Souslov *et al.* (2019), displayed in Table S-III, Case I yields $\tilde{c}_I = 7.48$ (since $\Omega\nu_o < 0$) and Case III yields $\tilde{c}_{III} = 8.48$ ($\Omega\nu_o > 0$). A disturbance propagating with a speed lying between these two values, moves with supersonic speed in the medium of case I, while it moves with subsonic speed in the medium of case III. Supersonic flow is distinctly different from subsonic flow. A disturbance of the latter eventually reaches every point in the medium and the presence of an obstacle will affect the (subsonic) flow both upstream and downstream.

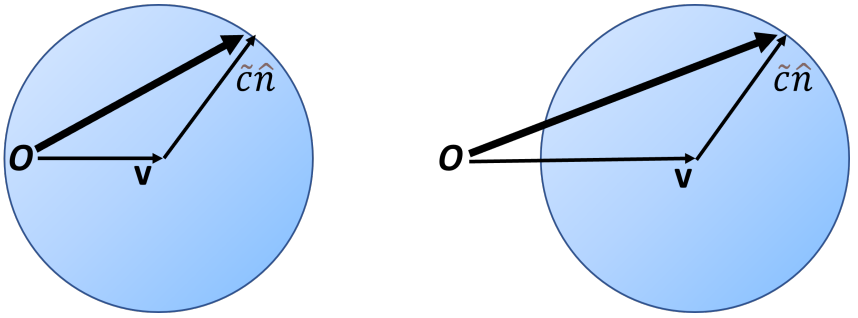

Figure S-XIV: A disturbance at a point O felt by a uniform flow of compressible rigidly-rotating odd viscous liquid with constant velocity $\mathbf{v}$ propagates with velocity $\mathbf{v} + \tilde{c}\hat{\mathbf{n}}$, where $\hat{\mathbf{n}}$ is an arbitrary unit vector (since the disturbance propagates relative to the liquid with the speed of sound $\tilde{c}$ in any direction cf. (Landau & Lifshitz 1987, §82)). **Left panel:** Explanation of scattering behaviour of topological waves from an obstacle (Souslov *et al.* 2019) (Case III, Table S-III). A subsonic disturbance ($v < \tilde{c}$) at point O propagates with velocity $\mathbf{v} + \tilde{c}\hat{\mathbf{n}}$ along the surface of the sphere depicted on the left, and eventually reaches any point in the medium ($\mathbf{v}$ is the velocity of the medium, $\hat{\mathbf{n}}$ a unit vector and $\tilde{c}$ the renormalized speed of sound defined in Eq. (S14)). Thus, a subsonic flow meeting an obstacle will be affected both upstream and downstream. **Right panel:** Explanation of non-scattering behaviour of topological waves from an obstacle (Souslov *et al.* 2019) (Case I, Table S-III). A supersonic disturbance $v > \tilde{c}$ at point O can only propagate downstream within the cone depicted on the right panel and thus, supersonic flow meeting an obstacle will only propagate downstream. Compare with (Landau & Lifshitz 1987, Fig. 50).

On the other hand, a disturbance in supersonic flow propagates only downstream and lies within a cone, while the flow outside the cone remains unaffected. When supersonic flow meets an obstacle, it propagates downstream leaving the upstream region unaffected; the upstream region does not "know" about the presence of the obstacle. Fig. S-XIV displays these two distinctive behaviours and is adopted from (Landau & Lifshitz 1987, Fig. 50). These are predictions of linear analysis with axial symmetry and are expected to become somewhat modified in the presence of nonlinear and azimuthally-dependent fields. This is discussed now in terms of the liquid vorticity.

Finally, depending on the type of the liquid (whether shear viscosity is included or not) there will be a boundary layer that will bring a velocity component, increasing exponentially in the bulk abruptly, down to zero near the boundary. We do not discuss here the manner by which this decay will take place and it is left for future investigations.

REFERENCES

Batchelor, G.K. 1967 *An introduction to fluid dynamics*. Cambridge University Press.

Davidson, P.A. 2013 *Turbulence in rotating, stratified and electrically conducting fluids*. Cambridge University Press, Cambridge.

Ganeshan, S. & Abanov, A.G. 2017 Odd viscosity in two-dimensional incompressible fluids. *Physical Review Fluids* **2** (9), 094101.

Khain, T., Scheibner, C., Fruchart, M. & Vitelli, V. 2022 Stokes flows in three-dimensional fluids with odd and parity-violating viscosities. *Journal of Fluid Mechanics* **934**, A23.

Kirkinis, E. & Olvera de la Cruz, M. 2023 Taylor columns and inertial-like waves in a three-dimensional odd viscous liquid. *Journal of Fluid Mechanics* **973**, A30.

Kuznetsov, E.A. & Dias, F. 2011 Bifurcations of solitons and their stability. *Physics Reports* **507** (2-3), 43–105.

Landau, L. D. & Lifshitz, E. M. 1960 *Electrodynamics of Continuous Media*. Oxford: Pergamon Press.

Landau, L. D. & Lifshitz, E. M. 1980 *Course of theoretical physics. Vol. 5: Statistical physics*. Oxford: Pergamon Press.

Landau, L. D. & Lifshitz, E. M. 1987 *Fluid Mechanics. Course of Theoretical Physics, Vol. 6*. Pergamon Press Ltd., London-Paris.

Lapa, M.F. & Hughes, T.L. 2014 Swimming at low Reynolds number in fluids with odd, or Hall, viscosity. *Physical Review E* **89** (4), 043019.

Lifshitz, E. M. & Pitaevskii, L. P. 1981 *Course of theoretical physics. Vol. 10: Physical Kinetics*. Pergamon Press.

Lighthill, J. 1978 *Waves in Fluids*. Cambridge University Press.

Lowman, N.K. & Hoefer, M.A. 2013 Dispersive shock waves in viscously deformable media. *Journal of Fluid Mechanics* **718**, 524–557.

Markovich, T. & Lubensky, T.C. 2021 Odd viscosity in active matter: microscopic origin and 3d effects. *Physical Review Letters* **127** (4), 048001.

Ostrovsky, L.A. & Potapov, A.I. 1999 *Modulated Waves*. The Johns Hopkins University Press.

Souslov, A., Dasbiswas, K., Fruchart, M., Vaikuntanathan, S. & Vitelli, V. 2019 Topological waves in fluids with odd viscosity. *Physical Review Letters* **122** (12), 128001.

Sprenger, P. & Hoefer, M.A. 2017 Shock waves in dispersive hydrodynamics with nonconvex dispersion. *SIAM Journal on Applied Mathematics* **77** (1), 26–50.